A simple setup miniaturization with multiple benefits for Green Chemistry in nanoparticle synthesis

Jette K. Mathiesen,[a,‡] Susan R. Cooper,[a,‡] Andy S. Anker,[a] Tiffany L. Kinnibrugh,[b] Kirsten M. Ø. Jensen[a,] and Jonathan Quinson[a,*]*

a. Chemistry Department, University of Copenhagen, 5 Universitetsparken, 2100 Copenhagen, Denmark

b. X-ray Science Division, Advanced Photon Source, Argonne National Laboratory, Argonne, IL, 60439, USA

* Corresponding authors:

kirsten@chem.ku.dk +45 35 33 47 97

jonathan.quinson@chem.ku.dk + 45 50 28 89 74

KEYWORDS

Miniaturization, High throughput, Screening, Nanoparticles, Synthesis

ABSTRACT

The development of nanomaterials often relies on wet-chemical syntheses performed in reflux-setups using round-bottom-flasks. An alternative approach to synthesize nanomaterials is here presented that uses glass tubes designed for NMR analysis as reactors. This approach uses less solvent, uses less energy, generates less waste, provides safer conditions, is less prone to contamination and is compatible with high throughput screening. The benefits of this approach are illustrated by an *in breadth* study with the synthesis of gold, iridium, osmium and copper sulfide nanoparticles.

Introduction. Nanomaterials (NMs) are used in multiple applications ranging from catalysis, optics, medicine to water/air treatments.[1-3] Due to strong structure-property relations on the nanoscale, the careful and rational synthesis of NMs is important. Consequently, the controlled syntheses of NMs has been increasingly addressed as a key component of Green Chemistry.[4-8] The need for protocols generating less waste and increasing safety has been stressed.[6,7] A focus is often given to the solvents and reactants to select,[9] and the use of microwaves or ultrasound, considered more energy efficient.[8] The development of setups such as flow (micro)reactors is also useful to minimize waste and simplify NM synthesis.[10-12] However, ‘‘despite these advantages, microfluidic systems have yet to be extensively adopted by the colloidal nanomaterial community’’.[13] The above strategies often require specific equipment and expertise, which may account for their relatively limited implementation. Simpler miniaturized systems with high throughput potential would gain to be proposed.

Wet-chemical methods often show promising scalability while being easily implemented in most modern laboratories.[14-16] NMs with various compositions, sizes and structures can be prepared by wet-chemical syntheses, which results in tuned NM properties to best match specific requirements for various applications.[16-18] The control over NM features is achieved by tuning experimental parameters, e.g. temperature, concentration of reactants, type of reactants or solvent composition. However, studying and understanding how synthetic parameters influence the NMs produced is often limited by the time and resources required to make a single batch of NMs. In a textbook approach using reflux-setups, 10-100 mL of solvent is typically required and only one experiment can be performed every few hours and per setup, see **Scheme 1**. To understand how NM structures change with synthetic parameters, alternative high throughput strategies are needed.

As an alternative to the conventional reflux-setup, we here investigate the use of glass tubes designed for nuclear magnetic resonance (NMR) measurements as miniaturized reactors,[19,20] **Scheme 1** and details in the *Methods* section. The multiple advantages of this simple alternative in Green Chemistry for NM synthesis[6,8] are illustrated by an *in breadth* study with the preparation of four different nanoparticles (NPs): gold (Au), iridium (Ir), osmium (Os) and copper sulfide ($Cu_{2-x}S$). Although precious metal (PM) based NPs are made of non-renewable resources, they remain key materials in multiple applications,[7] e.g. to develop fossil-fuel-free technologies for energy conversion,[17] and as models to understand NM formation.[21] Even minor improvements in PM NP syntheses can have significant scientific, economic and ecologic impact.

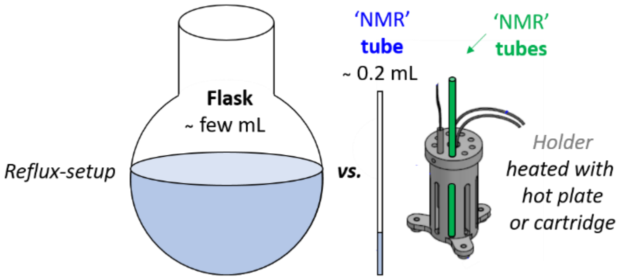

Scheme 1. Moving from *round-bottom-flask* to *NMR tube* glassware for greener NM syntheses and studies.

Results and Discussion

Au NPs. Au NPs have been a case study for Green Chemistry in NM synthesis.[7] In particular, the Turkevich synthesis is widely reported, where typically 0.1-0.5 mM $HAuCl_4$ is reduced in water close to the boiling point by trisodium tricitrate.[22,23] The investigation of the many parameters controlling the properties of the Au NPs[22] would gain from high throughput approaches using less solvent than the typical 200-500 mL required. The Au NPs obtained performing the Turkevich synthesis in 500 mL (reflux-setup) or 0.2 mL (NMR tube) lead to the same NP size ca. 13 nm within the error of measurement by TEM, **Figure 1**. A range of alternative Au NP syntheses use organic solvents such as oleylamine and relatively high temperature.[24] Syntheses at higher temperature, e.g. 200 °C, are possible since nut and ferrule can be used to close the NMR tube, **Figure 1C**.

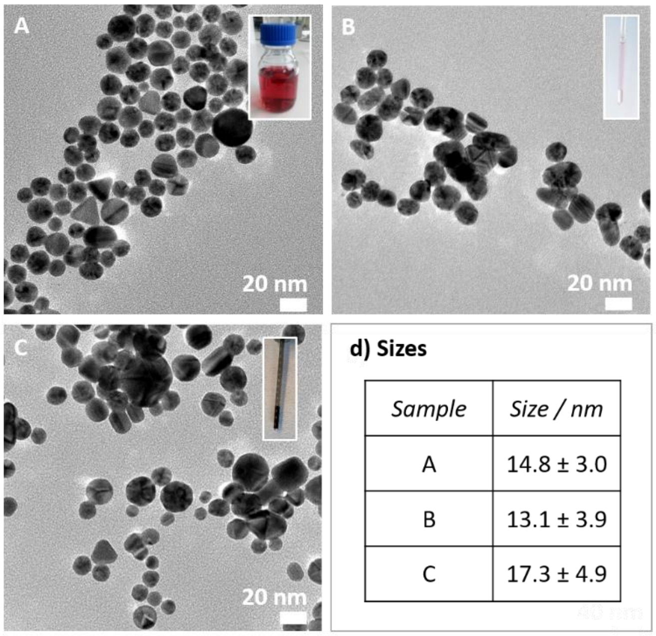

d) Sizes

Sample	*Size / nm*
A	14.8 ± 3.0
B	13.1 ± 3.9
C	17.3 ± 4.9

Figure 1. TEM micrographs of Au NPs obtained from 0.125 mM $HAuCl_4$ in water in presence of 2.2 mM trisodium citrate at 100 °C for 1 hour for a total volume of (A) 500 mL and (B) 0.2 mL. (C) TEM micrographs of Au NPs obtained using oleylamine at 200 °C as solvent in 0.3 mL. Insets are pictures of the resulting colloidal dispersions. TEM acquired at different magnifications and the related size distribution are available in Figure S1. (D) Table of the related size distributions.

Ir NPs. We reported a surfactant-free colloidal synthesis of PM NPs directly relevant for the industry,[17,25] performed at low temperature (< 80 °C) in alkaline mono-alcohols like methanol or ethanol, leading to high catalytic activity for the oxygen evolution reaction,[17,26] without intensive washing or purification steps, thus already addressing few Green Chemistry principles for NP synthesis.[6,7,27] The Ir NPs are in the range 1-2 nm across a wide range of experimental parameters.[28] To possibly achieve size control, investigating high concentrations of precursor and long synthesis time are reasonable options. Using a microwave or even a classical reflux-setup, it is arguably challenging to investigate these hypotheses due to safety concerns, higher precursor cost and pressure on lab space and equipment access.

Using NMR tubes, safe and simple time resolved studies over weeks of synthesis using high precursor concentrations (100 mM $IrCl_3$) are easily performed, see **Figure 2**. In line with previous reports using microwave synthesis[17] or UV-vis induced synthesis[28] it is found that Ir NPs with an average size of 1.6 nm are obtained. A significant achievement here is that the NPs are obtained at high concentration (100 mM) of precursor. This result underlines the relevance of this recently reported Ir NP synthesis to scale up the synthesis of extremely active catalysts for the oxygen reduction reaction.[17,29]

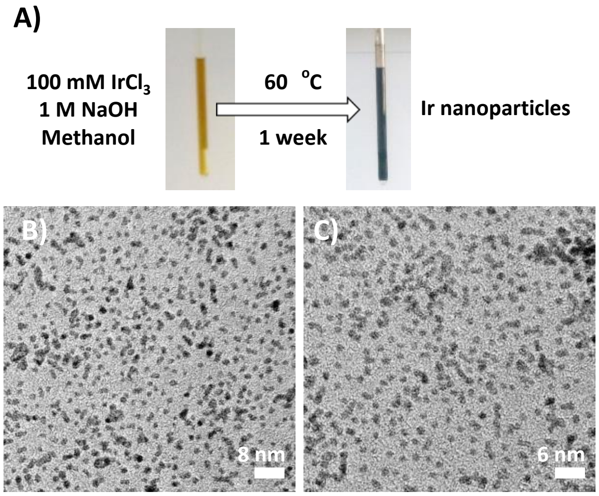

Figure 2. (A) General conditions for Ir NP synthesis. The NMR tube is 3 mm in diameter and the magnetic stirrer bar is 1.5 mm long. (B-C) TEM micrographs at different magnifications of Ir NPs obtained from 100 mM $IrCl_3$ in 1 M NaOH in methanol at 60 °C for a week for a total volume of 0.2 mL. See also Figures S2-S3.

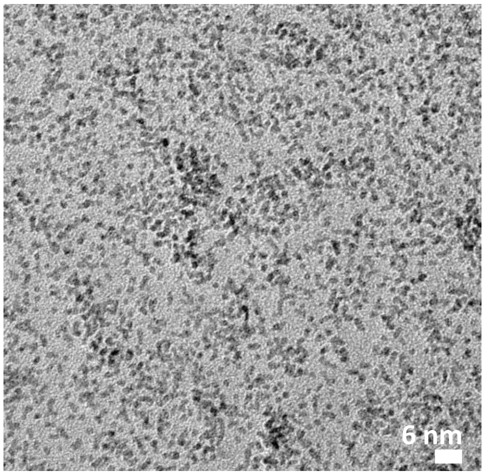

Figure 3. TEM micrographs of Os NPs obtained from 100 mM $OsCl_3$ in methanol:water (1:2, v:v) at 85 °C for a week, for a total volume of 0.2 mL. Size distribution are available in Figure S4.

Os NPs. Os NP synthesis has received less attention than other PMs.[30-32] Taking advantage of the small volume of solvent needed, we investigated the surfactant-free synthesis of Os NPs using a high precursor concentration in simple low boiling points solvents such as a mixture of methanol and water. TEM micrograph of the resulting materials obtained for a one-week long synthesis starting with 100 mM of $OsCl_3$ show that small size NPs, ca. 1.6 ± 0.4 nm in diameter, are obtained **Figures 3**. Although Os NPs are made of non-earth abundant element, the small size Os NPs obtained by a surfactant-free approach are relevant to develop more sustainable energy conversion systems to move away from fossil-fuels based energy.[33-35]

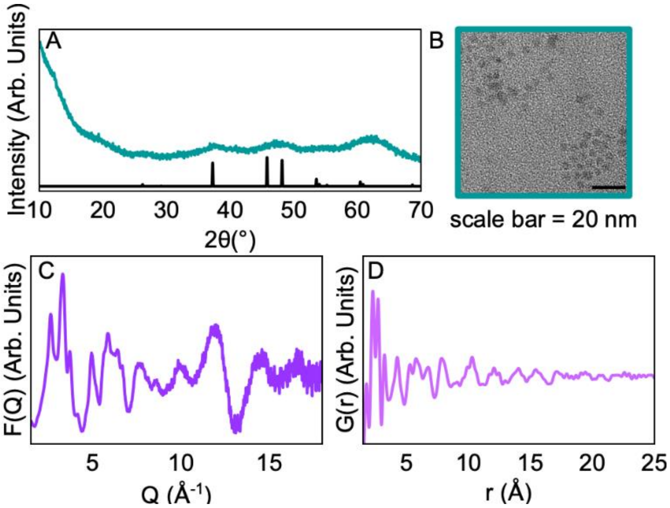

Figure 4. Characterization of Cu$_{2-x}$S NPs obtained in an NMR tube setup. (A) Using a lab-source XRD instrument (blue) compared to a calculated diffraction pattern of β-chalcocite taking the space group P6$_3$/mmc (black). (B) TEM micrographs of the washed NPs. (C) F(Q) and (D) PDF (G(r)) of X-ray total scattering data.

Cu$_{2-x}$S NPs. Cu$_{2-x}$S NPs have applications in batteries,[36,37] sensors[38] and as an oxygen evolution reaction catalyst.[39] The analysis with a lab-source XRD instrument of the NPs synthesized in the NMR tubes suggests that small Cu$_{2-x}$S NPs were formed, **Figure 4A**. TEM analysis shows a size of 4.5 ± 0.9 nm, **Figure 4B** and **Figure S5**. While some features are observed in the XRD pattern in **Figure 4A**, the broadening of Bragg peaks from these small NPs makes any structural investigation challenging. In contrast, the use of the NMR tube makes further characterization straightforward, e.g. using synchrotron scattering techniques, as many measurements can be done directly on the sample in the NMR tube. For instance, the as-prepared samples in closed NMR tubes can be sent to synchrotron for X-ray total scattering with pair distribution function (PDF) analysis. The PDF can be understood as a histogram of atom-atom distances in the material. In **Figure 4C,D** are reported the F(Q) (data in reciprocal space) and G(r) (data in real space) of the reaction solution after background subtraction. The PDF analysis confirm that the NPs can be described by a β-chalcocite model in space group $P6_3/mmc$[40] with deviations in the local structure, **Figure S6**. Furthermore, the structure obtained is the same whether the reaction is performed in the NMR setup or a conventional reflux setup.

Benefits. The use of NMR tubes readily lead to several advantages in terms of synthesis strategy. Using 3 mm diameter NMR tubes, allows to perform syntheses with volume as low as 0.1 mL, **Figure 2**. This low volume reduces the amount of waste generated and allows investigating the effect of high concentration solutions towards scaling-up.[7,16] Sample holders can be designed to perform several experiments at a time (up to 9 experiments per holder in the current design, **Figure S7**) allowing high throughput screening while requiring minimal lab space. Small volume also allows safer operating conditions. As a result, both long(er) and an increased number of experiments can be performed with little equipment required, while optimizing the energy needed to heat up the solutions. Temperature control is achieved by either using the temperature control of a heating plate or using dedicated heating cartridge with a temperature controller to control the heating rate, **Figures 5** in the *Methods* section. Septa can be used to close the NMR tubes to control the atmosphere, alternatively, nut and ferrules can be used for higher pressure experiments. The length of the NMR tube provides an area of contact with cool air to function under reflux conditions. This area can also be cooled down, e.g. with a fan or dedicated water-cooling devices. It is worth stressing that the synthesis can be performed with stirring by simply using a commercially available stirrer bar (e.g. 8 mm x 1.5 mm) in the NMR tube, **Figure 2**.

Further considerations. NMR tubes have previously been used as reactors for *in situ* studies at synchrotrons or for NMR characterization.[20,41] However, they have often been used not as a preferred reaction vessel but to make the experiment compatible with a given type of measurement, e.g. NMR. The experimental conditions selected to perform these specific experiments are often the results of screening performed on larger scale syntheses. A drawback of screening studies developed and optimized in laboratories is thus that they are often challenging to directly adapt to the requirements and limitations of synchrotron setups. For example, PDF measurements are best performed on samples with high concentration of the material of interest, especially when considering poorly scattering elements like transition metal sulfides. Here, the NMR tube setup offers the option to readily investigate high concentration of materials during parametric studies performed in home laboratories (outside synchrotrons facilities). Ultimately, this allows comparing more directly selected measurements performed at synchrotron facilities with larger screening experiments done in a chemistry lab. This further enables researchers to design experiments for even more complex *in situ* analysis of various reactions.[19,42,43]

NMR tubes make it possible to use a clean vessel for each experiment. This alleviates the need to clean glassware, thus limiting the chemical waste generation related to cleaning steps, e.g. using *aqua regia* for Au NPs.[44] Importantly, it alleviates the question of cross contamination, thus addressing the well-known issue of reproducibility in NM science, often ascribed to chemical impurities from various sources.[45] NM synthesis can be sensitive to variations of room temperature or room light, and the stability overtime of the chemicals and/or precursors solutions can be an issue.[46] These variables may be challenging to control across long periods of time when a study would last for instance several weeks of months. This drawback is alleviated with NMR tubes as reactors since several experiments including controls can be performed at the same time. Energy is saved because several experiments are heated all at once. The ease of simply performing relatively long experiments is also a positive feature towards improved yield of the precursor conversion to NMs.

It could be argued that due to the small diameter of the NMR tubes, capillary effects might come into play and the actual temperature-pressure during reaction might not be well-known. This issue of variability in physical parameters of reactors, e.g. heat transfer properties, stirring etc., is the same for most scaling up to date, e.g. when moving from reflux-setups to larger scale reactors. In this respect, the use of NMR tubes reactors remains a convenient and *green* approach to (pre)screen the influence of experimental parameters.

A final practical consideration is storage and reuse. The small NMR tubes are easily stored due to their small diameter and length. The 18 cm long NMR tube are easily cut with a commercially available glasscutter to save more space. The open end of the glass can be sealed by melting with a torch (e.g. butane torch), for instance when toxic reagents and/or air sensitive compounds are involved. The samples can be safely and space-efficiently stored for further analysis. Additionally, the cut section of the NMR tube can be cleaned and sealed by melting one extremity to be re-used as a new miniaturized vessel.

Conclusions. A simple alternative to the classical round-bottom flask synthesis approach to prepare NMs is presented. An *in breadth* study of four different nanomaterials is presented covering gold, iridium, osmium and copper sulfide nanomaterials. The general approach is relevant for the synthesis of other nanomaterials like palladium, platinum or silver that would be performed in similar solvent and/or for the same temperature range.[17,47] By using commercially available NMR tubes, a miniaturized vessel suitable for the synthesis of various NMs is readily obtained. This approach complies with several of the principles of Green Chemistry for NM synthesis.[6,7]

This approach is therefore directly relevant for academic research and research and development but also educational purposes.

With the increasing interest in machine learning and artificial intelligence, large datasets are needed to feed algorithms.[48] The present approach allows for high throughput (pre)screening. Multi-technique characterization remains a general limiting factor in nanoscience[49] but the expected improvements in this area of research are promising.[6,19,41,50] If characterization was kept minimal in this *in breadth* approach, enough material is still obtained for characterization by TEM, XRD or PDF and naturally NMR, high resolution TEM or UV-vis characterization with an appropriate setup. It is expected that the simple alternative proposed here will also be relevant for various syntheses of molecules and other chemical reactions.

Methods

Chemicals

All chemicals were used as received: $HAuCl_4{\cdot}3H_2O$ (≥99.9% trace metals basis Merck); trisodium citrate (99%, Alfa Aesar); $IrCl_3$ (99.8%, metals basis, Alfa Aesar); $OsCl_3{\cdot}xH_2O$ (Sigma-Aldrich); NaOH (ACS, Reag. EMSURE®, Merck); methanol (≥99.9%, HiPerSolv Chromanorm®, VWR); water (Milli-Q, Millipore, resistivity >18.2 MΩ·cm, total organic carbon (TOC) <5 ppb); oleylamine (OLA, 70%, technical grade, Sigma Aldrich); gold(III) acetate (Au(ac)3, 99.9% metal basis, Alfa Aesar); 1-dodecanethiol (>98%, Sigma), n-Hexane (≥97%, HiPerSolv CHROMANORM®, VWR), oleic acid (90% Technical grade, Sigma), Cu(II) acetate (99% trace metals basis, Sigma), acetone (Chemex Products Aps).

Materials

NMR tubes (Wildmad®, 3 mm outer diameter, 0.27 mm wall thickness, Type 1 Class A); magnets (Fisherbrand PTFE Stirrer bar, 8 mm x 1.5 mm); Copper or nickel transmission electron microscope (TEM) grids (Quantifoil or Agar Scientific), were all used as received. The synthesis was performed in the configurations detailed below in **Figure 5** using a homemade NMR tube holder detailed in **Figure S7**. It can also be performed by placing the NMR tubes in a temperature controlled water or oil bath.

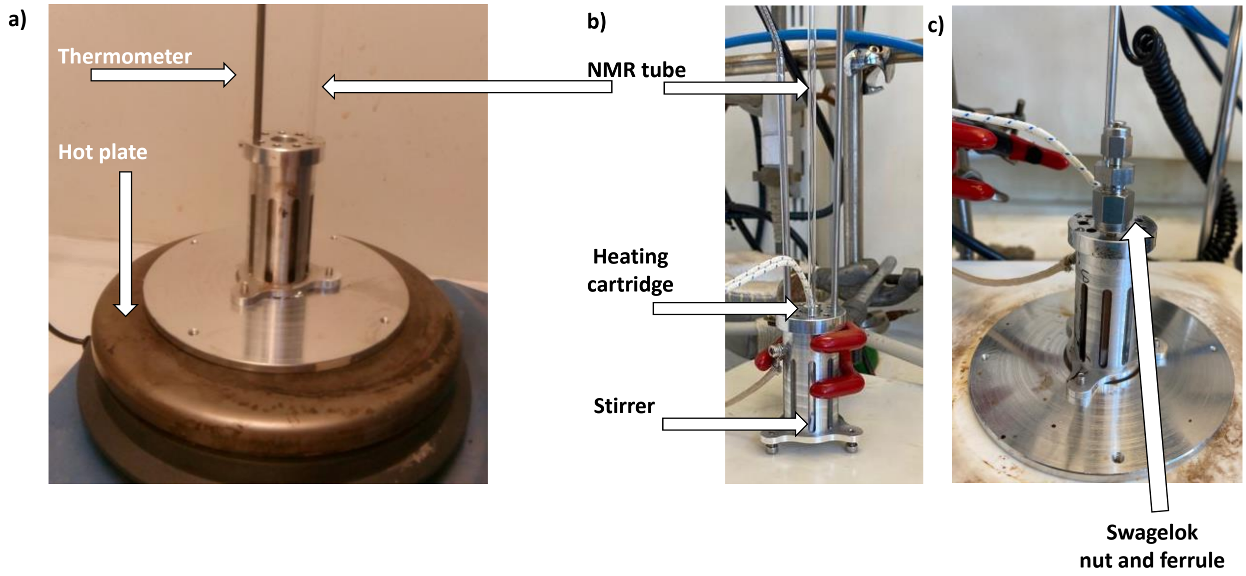

Figure 5. Photographs of different setups using a 3 mm NMR tube as reaction vessel (a) using a hot plate, (b) using a heating cartridge, (c) using a Swagelok nut and ferrule. The stirrer bar is 1.5 mm long, the NMR tube 3 mm in diameter. See technical details in Figure S7.

Syntheses.

Note: Some reactions can be dangerous, here in particular the synthesis of Os nanoparticles (NPs), since OsO_4 can easily form and is highly toxic. The synthesis must be performed in a fume-cupboard. Conveniently, the synthesis can be performed in NMR tubes closed with a cap (red cap provided upon buying the NMR tubes, or further septa fitting the NMR tubes can be purchased: *Precision seal rubber setpa cap (for 3 mm OD tubes and ampoules) pack of 100 ea*) and further sealed with Parafilm®. Alternatively, the NMR tube can be melted and sealed for the experiment or at the end of the experiments, e.g. with a butane torch. Otherwise nuts and ferrules (Swagelok) can be used. These opportunities to seal the vessel are also relevant for further storage.

Au NP synthesis. The Au NPs were obtained following the general procedure for the Turkevitch synthesis.[22,23] The Au NPs were produced from a mixture of 0.125 mM $HAuCl_4$ with 2.2 mM trisodium citrate in water, for a total volume of 500 mL in a reflux setup or 0.2 mL in a 3 mm diameter NMR tube. The solution containing trisodium citrate was pre-heated at 100 °C before the gold-containing solution was added (the volume before gold injection was 499 mL or 0.1 mL). In both cases, a hot plate was used to heat up the solution to 100 °C and the reaction after adding gold was left to pursue for 1 hour at this temperature of 100 °C with a stirring rate set at 1000 rotation per minutes.

Alternatively, the Au NPs were obtained using organic solvents.[24,51] To a glass vial, 9 mL oleylamine (OLA) and 25 mM $Au(ac)_3$ were added. The precursor solution was heated to 50 °C under air, while stirring at 400 rotation per minutes (rpms) until the metal ion precursor was dissolved. 4.5 mL of the precursor solution was taken to a separate vial, into which 25 μL dodecanethiol (DDT) was added and further heated to 50 °C under air, while stirring at 400 rpms. 0.3 mL of the solution was added to an NMR tube and closed by a Swagelok nuts and ferrules. The NMR tube was placed in the heating block, where the solution was heated to 200 °C at a heating rate of 7 °C min^{-1} and maintained at this temperature for 1 hour. The solution was cooled to room temperature. The resulting solution was added to a centrifuge tube with 20 mL hexane and was spun at 10 000 rpms for 10 minutes to precipitate the NPs. The particles were washed with a 3:1 ratio of ethanol: hexane three times. The particles were then suspended in 5 mL of hexane for future use.

Ir NP synthesis. The Ir NPs were obtained following the general procedure previously reported.[17,28,52] A mixture of 100 mM $IrCl_3$ in 1 M NaOH in methanol for a total volume of 0.2 mL was placed in a 3 mm diameter NMR tubes with a magnetic stirrer bar. The filled NMR tube was placed in a dedicated holder as presented in **Scheme 1** and **Figure 5**. A hot plate was used to heat up the miniaturized vessel to 60 °C for up to 1 week with a stirring set at 1000 rotation per minutes. The solution, which is initially light brown, turns black over time, see **Figure 2**.

Note: We previously used 4.4 mM in 10 mL[17] or 27 mL[52] to get enough mass of iridium, 8.5 mg and 23 mg respectively, for electrochemical testing. Using here ca. 20 times less solvent, the same mass of Ir NPs can be obtained due to the high concentration used.

Os NP synthesis. The Os NPs were obtained from a mixture of 100 mM $OsCl_3$ in methanol:water (1:2; v:v) for a total volume of 0.2 mL placed in a 3 mm diameter NMR tube with a magnetic stirrer bar. The filled NMR tube was placed in a dedicated holder as presented in **Scheme 1** and **Figure 5**. A hot plate was used to heat up the miniaturized vessel to 85 °C for 1 week with a stirring set at 1000 rotation per minutes.

$Cu_{2-x}S$ NP synthesis. To form copper sulfide NPs, a synthesis reported in the literature was modified.[53] A copper oleate precursor was obtained by heating 1 mmol of Cu(II) acetate with 2 mL of oleic acid in an oil bath at 150 °C for 1 hour. To 2 mL of copper oleate, 0.2 mL DDT was added, resulting in a viscous white precipitate. The mixture was mixed using a table-top vortex to ensure solution homogeneity. The copper oleate and DDT mixture was then added to 9.5 cm x 3 mm NMR tubes (obtained after cutting the initially 18 cm long tubes with a glasscutter) with approximately 0.25 mL using a needle and luer lock syringe. The NMR tubes were filled with N_2 and capped with a 3 mm silicone septa. The bottom of the septa was secured with epoxy and then wrapped in Teflon tape. The NMR tubes were then put into the heating setup equipped with a heating cartridge and a type J thermocouple that were plugged into a Cole parmer Digitroll II temperature controller. The samples were heated with a ramp rate of 185 °C h^{-1} to a final temperature of 200 °C and held at 200 °C for 3 hours before being cooled to room temperature. Two identical samples were prepared in NMR tubes so that three different analyses could be done: lab-source XRD, TEM and PDF analysis of X-ray total scattering data collected at 11-ID-B at Argonne National lab. Therefore, the NPs in one of the NMR tubes were washed by transferring the reaction liquid using a needle and a luer lock syringe to a 50 mL centrifuge tube. Approximately 5 mL of hexanes was used to rinse the NMR tube to ensure that as much of the reaction liquid as possible was transferred for washing. Acetone was then added to the NMR tube and it was centrifuged for 10 min at 9000 rpm. Particles were redispersed in hexanes and then washed one more time with acetone for 5 min and again with ethanol for 10 minutes before lab-source XRD and TEM analysis.

***Characterisation*.**

TEM microscopy. TEM microscopy was performed on a JEOL 2100 operated at 200 kV. The as prepared or washed Au, Ir, Os or $Cu_{2-x}S$ NP dispersions were dropped on TEM grids and images recorded in at least three different and randomly selected areas of the grids at least at three different magnifications. The size of the NPs was evaluated by measuring the diameter of at least 100 individual NPs for each sample using the software ImageJ.

Powder X-ray diffraction. The $Cu_{2-x}S$ NPs were dispersed in hexanes and drop cast onto a zero-background substrate for analysis on a Bruker D8 diffractometer with a Cu anode equipped with a Ni filter. The powder diffraction data was collected in Bragg-Bretano geometry from 10-70 degrees 2θ.

X-ray total scattering measurements. Data were measured at the 11-ID-B beamline at Argonne National Laboratory. Measurements were done using the beamline mail-in programme and remote beamline operation due to the Covid-19 pandemic. The samples were shipped from Copenhagen, Denmark to Argonne National Lab, USA in the NMR tube closed with a silicone septum, sealed with epoxy and Teflon tape. A sample for subtraction of the signal from the solvent was prepared by mixing 1.8 mL oleic acid and 0.2 mL of DDT and filled in NMR tubes. The reaction solution, solvent sample and an empty capillary were placed in an aluminum block for data collection at room temperature. The X-ray wavelength was 0.2115 Å and data were collected using a Perkin Elmer detector (200 um x 200 um pixel size) with a detector distance of 183.5 mm. Data were collected on the empty capillary, solvent and sample for 5 min. The data were integrated using Fit2D.[54] The data obtained from the glass capillary were subtracted from the data obtained from the reaction solution and solvent samples before using xPDFsuite[55,56] to subtract the signal from the solvent from the reaction solution and generate the PDF. A Q_{max} instrument of 18.5 $Å^{-1}$, Q_{max} 18 $Å^{-1}$, Q_{min} 1.5 $Å^{-1}$, and r_{poly} 1.1 were used to generate the PDF.

PDF refinements. CeO_2 was used for the calibration for detector distance as well as to determine the Q_{broad} and Q_{damp} parameters of the instrument. The PDF from the CeO_2 standard was modelled in the range from 1.3 Å to 60 Å with a Q_{broad} value of 0.0385 $Å^{-1}$ and Q_{damp} value of 0.0373 $Å^{-1}$ using the CeO_2 crystal structure model. Modelling of the sample PDF was done using PDFgui using the β-chalcocite structural model in space group $P6_3/mmc$. Below are **Tables S1-S2** of refined parameters. Two refinements were done at two different r-ranges. The first was done using the chalcocite structural model refined to the PDF in the range 2 Å to 30 Å, **Table S1**. The second was done using the chalcocite structural model refined to the PDF in the range 5.6 to 30 Å. The delta2 parameter (describing correlated motion) and $sp_{diameter}$ were fixed at values refined in the first refinement, **Table S2**.

ASSOCIATED CONTENT

Supporting Information.

The following files are available free of charge. TEM and PDF characterization, Sample holder specification, Figure S1-S7, Further discussion (PDF).

AUTHOR INFORMATION

Corresponding Author

* kirsten@chem.ku.dk, jonathan.quinson@chem.ku.dk

Author Contributions

The manuscript was written through contributions of all authors. All authors have given approval to the final version of the manuscript. ‡These authors contributed equally.

Funding Sources

This project has received funding from the European Union's Horizon 2020 research and innovation programme under the Marie Sklodowska-Curie grant agreement No. 840523 (CoSolCat, JQ) and 841903 (SRC). This project has received funding from the Villum

Foundation through a Villum Young Investigator grant (VKR00015416); the Danish National Research Foundation (DNRF 149) Center for High-Entropy Alloy Catalysis (CHEAC). This research used resources of the Advanced Photon Source, a U.S. Department of Energy (DOE) Office of Science User Facility, operated for the DOE Office of Science by Argonne National Laboratory under Contract No. DE-AC02-06CH11357 (GUP-73929).

ACKNOWLEDGMENT

E.T.S. Kjær, B. Wang, O. Aalling-Frederiksen, R. Pittkowski, University of Copenhagen, Denmark, H-C. Lu, University of Texas at Austin, USA, and beamline scientists O.J. Borkiewicz and L.C. Gallington are thanked for their help on synchrotron beamtime. S.B. Simonsen and L. Theil Kuhn, Technical University of Denmark, Denmark, are thanked for access to TEM facilities. Morten Liborius Jensen from the University of Copenhagen workshop is thanked for his help on the cell holder design and manufacturing.

REFERENCES

1 Cargnello, M. Colloidal Nanocrystals as Building Blocks for Well-Defined Heterogeneous Catalysts. *Chemistry of Materials* **31**, 576-596, doi:10.1021/acs.chemmater.8b04533 (2019).

2 Kalus, M. R., Rehbock, C., Barsch, N. & Barcikowski, S. Colloids created by light: Laser-generated nanoparticles for applications in biology and medicine. *Materials Today-Proceedings* **4**, S93-S100 (2017).

3 Chaudhary, S., Sharma, P., Chauhan, P., Kumar, R. & Umar, A. Functionalized nanomaterials: a new avenue for mitigating environmental problems. *International*

Journal of Environmental Science and Technology **16**, 5331-5358, doi:10.1007/s13762-019-02253-2 (2019).

4 Schmidt, J., Marques, M. R. G., Botti, S. & Marques, M. A. L. Recent advances and applications of machine learning in solid-state materials science. *Npj Computational Materials* **5**, doi:10.1038/s41524-019-0221-0 (2019).

5 Dhand, C. *et al.* Methods and strategies for the synthesis of diverse nanoparticles and their applications: a comprehensive overview. *Rsc Advances* **5**, 105003-105037, doi:10.1039/c5ra19388e (2015).

6 Hutchison, J. E. The Road to Sustainable Nanotechnology: Challenges, Progress and Opportunities. *Acs Sustainable Chemistry & Engineering* **4**, 5907-5914, doi:10.1021/acssuschemeng.6b02121 (2016).

7 Gilbertson, L. M., Zimmerman, J. B., Plata, D. L., Hutchison, J. E. & Anastas, P. T. Designing nanomaterials to maximize performance and minimize undesirable implications guided by the Principles of Green Chemistry. *Chemical Society Reviews* **44**, 5758-5777, doi:10.1039/c4cs00445k (2015).

8 Duan, H. H., Wang, D. S. & Li, Y. D. Green chemistry for nanoparticle synthesis. *Chemical Society Reviews* **44**, 5778-5792, doi:10.1039/c4cs00363b (2015).

9 Prat, D. *et al.* CHEM21 selection guide of classical- and less classical-solvents. *Green Chemistry* **18**, 288-296, doi:10.1039/c5gc01008j (2016).

10 Sui, J. S., Yan, J. Y., Liu, D., Wang, K. & Luo, G. S. Continuous Synthesis of Nanocrystals via Flow Chemistry Technology. *Small* **16**, doi:10.1002/smll.201902828 (2020).

11 Suryawanshi, P. L., Gumfekar, S. P., Bhanvase, B. A., Sonawane, S. H. & Pimplapure, M. S. A review on microreactors: Reactor fabrication, design, and cutting-edge applications. *Chemical Engineering Science* **189**, 431-448, doi:10.1016/j.ces.2018.03.026 (2018).

12 Damilos, S. *et al.* Continuous citrate-capped gold nanoparticle synthesis in a two-phase flow reactor. *Journal of Flow Chemistry*, doi:10.1007/s41981-021-00172-3.

13 Volk, A. A., Epps, R. W. & Abolhasani, M. Accelerated Development of Colloidal Nanomaterials Enabled by Modular Microfluidic Reactors: Toward Autonomous Robotic Experimentation. *Advanced Materials*, doi:10.1002/adma.202004495.

14 Saldanha, P. L., Lesnyak, V. & Manna, L. Large scale syntheses of colloidal nanomaterials. *Nano Today* **12**, 46-63, doi:10.1016/j.nantod.2016.12.001 (2017).

15 van Embden, J., Chesman, A. S. R. & Jasieniak, J. J. The Heat-Up Synthesis of Colloidal Nanocrystals. *Chemistry of Materials* **27**, 2246-2285, doi:10.1021/cm5028964 (2015).

16 Quinson, J. & Jensen, K. M. O. From platinum atoms in molecules to colloidal nanoparticles: A review on reduction, nucleation and growth mechanisms. *Advances in Colloid and Interface Science* **286**, doi:10.1016/j.cis.2020.102300 (2020).

17 Quinson, J. *et al.* Colloids for Catalysts: A Concept for the Preparation of Superior Catalysts of Industrial Relevance. *Angewandte Chemie-International Edition* **57**, 12338-12341, doi:10.1002/anie.201807450 (2018).

18 Losch, P. *et al.* Colloidal nanocrystals for heterogeneous catalysis. *Nano Today* **24**, 15-47, doi:10.1016/j.nantod.2018.12.002 (2019).

19 Marbella, L. E. & Millstone, J. E. NMR Techniques for Noble Metal Nanoparticles. *Chemistry of Materials* **27**, 2721-2739, doi:10.1021/cm504809c (2015).

20 Mateo, J. M. *et al.* Insights into the mechanism of the formation of noble metal nanoparticles byin situNMR spectroscopy. *Nanoscale Advances* **2**, 3954-3962, doi:10.1039/d0na00159g (2020).

21 Handwerk, D. R., Shipman, P. D., Whitehead, C. B., Ozkar, S. & Finke, R. G. Mechanism-Enabled Population Balance Modeling of Particle Formation en Route to Particle Average Size and Size Distribution Understanding and Control. *Journal of the American Chemical Society* **141**, 15827-15839, doi:10.1021/jacs.9b06364 (2019).

22 Wuithschick, M. *et al.* Turkevich in New Robes: Key Questions Answered for the Most Common Gold Nanoparticle Synthesis. *Acs Nano* **9**, 7052-7071, doi:10.1021/acsnano.5b01579 (2015).

23 Turkevich, J., Stevenson, P. C. & Hillier, J. A study of the nucleation and growth processes in the synthesis of colloidal gold. *Discussions of the Faraday Society*, 55-&, doi:10.1039/df9511100055 (1951).

24 Hiramatsu, H. & Osterloh, F. E. A simple large-scale synthesis of nearly monodisperse gold and silver nanoparticles with adjustable sizes and with exchangeable surfactants. *Chemistry of Materials* **16**, 2509-2511, doi:10.1021/cm049532v (2004).

25 Quinson, J. *et al.* Monovalent Alkali Cations: Simple and Eco-Friendly Stabilizers for Surfactant-Free Precious Metal Nanoparticle Colloids. *ACS Sustainable Chemistry & Engineering* **7**, 13680-13686, doi:10.1021/acssuschemeng.9b00681 (2019).

26 Bizzotto, F. *et al.* Ir nanoparticles with ultrahigh dispersion as oxygen evolution reaction (OER) catalyst: synthesis and activity benchmarking. *Catalysis Science & Technology* **9**, 6345-6356, doi:10.1039/C9CY01728C (2019).

27 Quinson, J. *et al.* Controlled Synthesis of Surfactant-Free Water-Dispersible Colloidal Platinum Nanoparticles by the Co4Cat Process. *ChemSusChem* **12**, 1229-1239, doi:10.1002/cssc.201802897 (2019).

28 Quinson, J. *et al.* UV-induced syntheses of surfactant-free precious metal nanoparticles in alkaline methanol and ethanol. *Nanoscale Advances* **2**, 2288-2292, doi:10.1039/d0na00218f (2020).

29 Bizzotto, F., Quinson, J., Schröder, J., Zana, A. & Arenz, M. Surfactant-free colloidal strategies for highly dispersed and active supported IrO2 $_c$atalysts: Synthesis and performance evaluation for the oxygen evolution reaction. *Journal of Catalysis* **401**, 54-62 (2021).

30 Wakisaka, T. *et al.* Discovery of face-centred cubic Os nanoparticles. *Chemical Communications* **56**, 372-374, doi:10.1039/c9cc09192k (2020).

31 Hirai, H., Nakao, Y. & Toshima, N. Preparation of colloidal transistion-metals in polymers by reduction with alcohols or ethers. *Journal of Macromolecular Science-Chemistry* **A13**, 727-750, doi:10.1080/00222337908056685 (1979).

32 Pitto-Barry, A. *et al.* Synthesis and controlled growth of osmium nanoparticles by electron irradiation. *Dalton Transactions* **44**, 20308-20311, doi:10.1039/c5dt03205a (2015).

33 Lim, C. S. *et al.* Iridium- and Osmium-decorated Reduced Graphenes as Promising Catalysts for Hydrogen Evolution. *Chemphyschem* **16**, 1898-1905, doi:10.1002/cphc.201500174 (2015).

34 Lam, V. W. S. & Gyenge, E. L. High-performance osmium nanoparticle electrocatalyst for direct borohydride PEM fuel cell anodes. *Journal of the Electrochemical Society* **155**, B1155-B1160, doi:10.1149/1.2975191 (2008).

35 Danilovic, N. *et al.* Activity-Stability Trends for the Oxygen Evolution Reaction on Monometallic Oxides in Acidic Environments. *Journal of Physical Chemistry Letters* **5**, 2474-2478, doi:10.1021/jz501061n (2014).

36 Jian, K., Chen, Z. H. & Meng, X. B. CuS and Cu2S as Cathode Materials for Lithium Batteries: A Review. *Chemelectrochem* **6**, 2825-2840, doi:10.1002/celc.201900066 (2019).

37 Rui, X. H., Tan, H. T. & Yan, Q. Y. Nanostructured metal sulfides for energy storage. *Nanoscale* **6**, 9889-9924, doi:10.1039/c4nr03057e (2014).

38 Guo, M. R. *et al.* Plasmonic Semiconductor Nanocrystals as Chemical Sensors: Pb2+ Quantitation via Aggregation-Induced Plasmon Resonance Shift. *Plasmonics* **9**, 893-898, doi:10.1007/s11468-014-9694-3 (2014).

39 Wang, X. L. *et al.* Cu-Deficient Plasmonic Cu2-xS Nanoplate Electrocatalysts for Oxygen Reduction. *Acs Catalysis* **5**, 2534-2540, doi:10.1021/acscatal.5b00115 (2015).

40 Cava, R. J., Reidinger, F. & Wuensch, B. J. Mobile ion distribution and anharmonic thermal motion in fast ion conducting Cu_2S. *Solid State Ionics* **5**, 501-504, doi:10.1016/0167-2738(81)90302-7 (1981).

41 Mathiesen, J. K. *et al.* Insights from In Situ Studies on the Early Stages of Platinum Nanoparticle Formation. *Journal of Physical Chemistry Letters* **12**, 3224-3231, doi:10.1021/acs.jpclett.1c00241 (2021).

42 Mathiesen, J. K. *et al.* Insights from In Situ Studies on the Early Stages of Platinum Nanoparticle Formation. *J. Phys. Chem. Lett.* **12**, 3224–3231 (2021).

43 Wu, S. Y., Li, M. R. & Sun, Y. G. In Situ Synchrotron X-ray Characterization Shining Light on the Nucleation and Growth Kinetics of Colloidal Nanoparticles. *Angewandte Chemie-International Edition* **58**, 8987-8995, doi:10.1002/anie.201900690 (2019).

44 De Souza, C. D., Nogueira, B. R. & Rostelato, M. Review of the methodologies used in the synthesis gold nanoparticles by chemical reduction. *Journal of Alloys and Compounds* **798**, 714-740, doi:10.1016/j.jallcom.2019.05.153 (2019).

45 Liz-Marzan, L. M., Kagan, C. R. & Millstone, J. E. Reproducibility in Nanocrystal Synthesis? Watch Out for Impurities! *Acs Nano* **14**, 6359-6361, doi:10.1021/acsnano.0c04709 (2020).

46 Quinson, J. *et al.* Teaching old precursors new tricks: Fast room temperature synthesis of surfactant-free colloidal platinum nanoparticles. *Journal of Colloid and Interface Science* **577**, 319-328, doi:10.1016/j.jcis.2020.05.078 (2020).

47 Quinson, J. *et al.* Solvent-Dependent Growth and Stabilization Mechanisms of Surfactant-Free Colloidal Pt Nanoparticles. *Chemistry-a European Journal* **26**, 9012-9023, doi:10.1002/chem.202001553 (2020).

48 Kalinin, S. V., Sumpter, B. G. & Archibald, R. K. Big-deep-smart data in imaging for guiding materials design. *Nature Materials* **14**, 973-980, doi:10.1038/nmat4395 (2015).

49 Mourdikoudis, S., Pallares, R. M. & Thanh, N. T. K. Characterization techniques for nanoparticles: comparison and complementarity upon studying nanoparticle properties. *Nanoscale* **10**, 12871-12934, doi:10.1039/c8nr02278j (2018).

50 Modena, M. M., Ruhle, B., Burg, T. P. & Wuttke, S. Nanoparticle Characterization: What to Measure? *Advanced Materials* **31**, doi:10.1002/adma.201901556 (2019).

51 Fanizza, E. *et al.* A combined size sorting strategy for monodisperse plasmonic nanostructures. *Nanoscale* **5**, 3272-3282, doi:10.1039/c3nr33944k (2013).

52 Bizzotto, F. *et al.* Ir nanoparticles with ultrahigh dispersion as oxygen evolution reaction (OER) catalysts: synthesis and activity benchmarking. *Catalysis Science & Technology* **9**, 6345-6356, doi:10.1039/c9cy01728c (2019).

53 Choi, S. H. *et al.* Simple and Generalized Synthesis of Semiconducting Metal Sulfide Nanocrystals. *Advanced Functional Materials* **19**, 1645-1649, doi:10.1002/adfm.200800832 (2009).

54 Hammersley, A. P., Svensson, S. O., Hanfland, M., Fitch, A. N. & Hausermann, D. Two-dimensional detector software: From real detector to idealised image or two-theta scan. *High Pressure Research* **14**, 235-248, doi:10.1080/08957959608201408 (1996).

55 Yang, X., Juhas, P., Farrow, C. L. & Billinge, S. J. L. xPDFsuite: an end-to-end software solution for high throughput pair distribution function transformation, visualization and analysis. *arXiv:1402.3163 [cond-mat.mtrl-sci]* (2015).

56 Juhas, P., Davis, T., Farrow, C. L. & Billinge, S. J. L. PDFgetX3: a rapid and highly automatable program for processing powder diffraction data into total scattering pair distribution functions. *Journal of Applied Crystallography* **46**, 560-566, doi:10.1107/s0021889813005190 (2013).

TABLE OF CONTENT

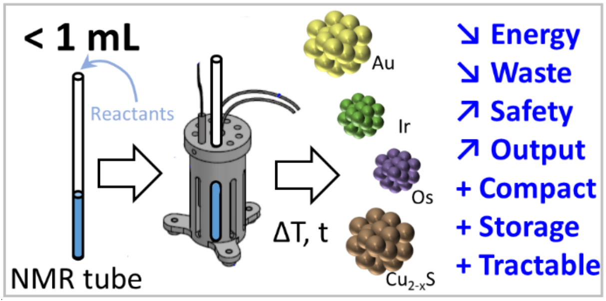

SYNOPSIS

Small diameter NMR tubes are ideal reactors to implement the Green Chemistry principles in wet-chemical nanomaterial synthesis studies.